

Measurements of the Solar Neutrino Flux from Super-Kamiokande's First 300 Days

The Super-Kamiokande Collaboration

Submitted to Phys. Rev. Lett.

Y.Fukuda^a, T.Hayakawa^a, E.Ichihara^a, K.Inoue^a, K.Ishihara^a, H.Ishino^a, Y.Itow^a, T.Kajita^a,
J.Kameda^a, S.Kasuga^a, K.Kobayashi^a, Y.Kobayashi^a, Y.Koshio^a, K.Martens^a, M.Miura^a,
M.Nakahata^a, S.Nakayama^a, A.Okada^a, M.Oketa^a, K.Okumura^a, M.Ota^a, N.Sakurai^a, M.Shiozawa^a,
Y.Suzuki^a, Y.Takeuchi^a, Y.Totsuka^a, S.Yamada^a, M.Earl^b, A.Habig^b, J.T.Hong^b, E.Kearns^b,
S.B.Kim^{b,1}, M.Masuzawa^{b,2}, M.D.Messier^b, K.Scholberg^b, J.L.Stone^b, L.R.Sulak^b, C.W.Walter^b,
M.Goldhaber^c, T.Barszczak^d, W.Gajewski^d, P.G.Halverson^{d,3}, J.Hsu^d, W.R.Kropp^d, L.R. Price^d,
F.Reines^d, H.W.Sobel^d, M.R.Vagins^d, K.S.Ganezer^e, W.E.Keig^e, R.W.Ellsworth^f, S.Tasaka^g,
J.W.Flanagan^{h,2}, A.Kibayashi^h, J.G.Learned^h, S.Matsuno^h, V.Stenger^h, D.Takemori^h, T.Ishiiⁱ,
J.Kanzakiⁱ, T.Kobayashiⁱ, K.Nakamuraⁱ, K.Nishikawaⁱ, Y.Oyamaⁱ, A.Sakaiⁱ, M.Sakudaⁱ, O.Sasakiⁱ,
S.Echigo^j, M.Kohama^j, A.T.Suzuki^j, T.J.Haines^{k,d}, E.Blaufuss^l, R.Sanford^l, R.Svoboda^l, M.L.Chen^m,
Z.Conner^{m,4}, J.A.Goodman^m, G.W.Sullivan^m, M.Mori^{n,5}, J.Hill^o, C.K.Jung^o, C.Mauger^o, C.McGrew^o,
E.Sharkey^o, B.Viren^o, C.Yanagisawa^o, W.Doki^p, T.Ishizuka^{p,6}, Y.Kitaguchi^p, H.Koga^p, K.Miyano^p,
H.Okazawa^p, C.Saji^p, M.Takahata^p, A.Kusano^q, Y.Nagashima^q, M.Takita^q, T.Yamaguchi^q, M.Yoshida^q,
M.Etoh^r, K.Fujita^r, A.Hasegawa^r, T.Hasegawa^r, S.Hatakeyama^r, T.Iwamoto^r, T.Kinebuchi^r, M.Koga^r,
T.Maruyama^r, H.Ogawa^r, A.Suzuki^r, F.Tsushima^r, M.Koshiba^s, M.Nemoto^t, K.Nishijima^t,
T.Futagami^u, Y.Hayato^u, Y.Kanaya^u, K.Kaneyuki^u, Y.Watanabe^u, D.Kielczewska^{v,d,7}, R.Doyle^w,
J.George^w, A.Stachyra^w, L.Wai^w, J.Wilkes^w, K.Young^w

^a*Institute for Cosmic Ray Research, University of Tokyo, Tanashi, Tokyo 188-8502, Japan*

^b*Department of Physics, Boston University, Boston, MA 02215, USA*

^c*Physics Department, Brookhaven National Laboratory, Upton, NY 11973, USA*

^d*Department of Physics and Astronomy, University of California, Irvine Irvine, CA 92697-4575, USA*

^e*Department of Physics, California State University, Dominguez Hills, Carson, CA 90747, USA*

^f*Department of Physics, George Mason University, Fairfax, VA 22030, USA*

^g*Department of Physics, Gifu University, Gifu, Gifu 501-1193, Japan*

^h*Department of Physics and Astronomy, University of Hawaii, Honolulu, HI 96822, USA*

ⁱ*Institute of Particle and Nuclear Studies, High Energy Accelerator Research Organization (KEK), Tsukuba, Ibaraki 305-0801, Japan*

^j*Department of Physics, Kobe University, Kobe, Hyogo 657-8501, Japan*

^k*Physics Division, P-23, Los Alamos National Laboratory, Los Alamos, NM 87544, USA.*

^l*Physics Department, Louisiana State University, Baton Rouge, LA 70803, USA*

^m*Department of Physics, University of Maryland, College Park, MD 20742, USA*

ⁿ*Department of Physics, Miyagi University of Education, Sendai, Miyagi 980-0845, Japan*

^o*Physics Department, State University of New York, Stony Brook, NY 11794-3800, USA*

^p*Department of Physics, Niigata University, Niigata, Niigata 950-2181, Japan*

^q*Department of Physics, Osaka University, Toyonaka, Osaka 560-0043, Japan*

^r*Department of Physics, Tohoku University, Sendai, Miyagi 980-8578, Japan*

^s*The University of Tokyo, Tokyo 113-0033, Japan*

¹Present address: Department of Physics, Seoul National University, Seoul 151-742, Korea

²Present address: Accelerator Laboratory, High Energy Accelerator Research Organization (KEK)

³Present address: NASA, JPL, Pasadena, CA 91109, USA

⁴Present address: Enrico Fermi Institute, University of Chicago, Chicago, IL 60637 USA

⁵Present address: Institute for Cosmic Ray Research, University of Tokyo

⁶Present address: Dept. of System Engineering, Shizuoka University Hamakita, Shizuoka 432-8561, Japan

⁷Supported by the Polish Committee for Scientific Research.

^tDepartment of Physics, Tokai University, Hiratsuka, Kanagawa 259-1292, Japan
^uDepartment of Physics, Tokyo Institute for Technology, Meguro, Tokyo 152-8551, Japan
^vInstitute of Experimental Physics, Warsaw University, 00-681 Warsaw, Poland
^wDepartment of Physics, University of Washington, Seattle, WA 98195-1560, USA

Abstract

The first results of the solar neutrino flux measurement from Super-Kamiokande are presented. The results shown here are obtained from data taken between the 31st of May, 1996, and the 23rd of June, 1997. Using our measurement of recoil electrons with energies above 6.5 MeV, we infer the total flux of ${}^8\text{B}$ solar neutrinos to be $2.42 \pm 0.06(\text{stat.}) \pm_{0.07}^{+0.10}(\text{syst.}) \times 10^6/\text{cm}^2/\text{s}$. This result is consistent with the Kamiokande measurement and is 36% of the flux predicted by the BP95 solar model. The flux is also measured in 1.5 month subsets and shown to be consistent with a constant rate.

The neutrino plays a crucial role in both astrophysics and particle physics. This report is on measurements of solar neutrinos that are produced in the core of the sun through nuclear reaction chains. Since neutrinos pass through matter largely unimpeded, the mechanism of solar energy generation taking place at the central core of the sun can be studied directly by solar neutrinos. Evidence of as yet unresolved neutrino properties may also be obtained by detailed studies of the solar neutrinos, as these neutrinos are produced in very dense matter, pass through the core and surrounding layers to the surface of the star, and reach the Earth after about 150 million kilometers of flight. This naturally-arranged situation enables us to study possible neutrino mass and magnetic properties.

Tens of billions of neutrinos from the sun traverse each square centimeter of the Earth every second. Four different experiments [1, 2, 3, 4, 5] have detected these neutrinos. All of the experiments have observed a significantly lower flux than that predicted by standard solar models (SSMs)[6, 7, 8]. This discrepancy, first suggested by the historic Cl-experiment[1], is called “the solar neutrino problem.” One of the characteristics of the problem is that the amount of suppression among the experiments appears to be energy-dependent. Detailed studies of this phenomenon strongly suggest that these deficits are not easily explained by changing solar models, but can be naturally explained by neutrino oscillations[9].

Super-Kamiokande is capable of observing direct and solar-model-independent evidence of neutrino oscillations. Observation of a distortion of the recoil electron energy spectrum, short-term time variations (like the daytime and nighttime flux difference), and the time variation associated with the solar activity cycle, would constitute such evidence. The production of solar neutrinos is supposed to be stable over a time scale of several million years, and if any time variations were to be found, that would indicate either neutrino mass and mixing[10], or the presence of non-zero neutrino magnetic moments[11]. Such solar-model-independent studies require small statistical and systematic errors, which in turn require long-term data accumulation.

In this letter, we present the first results of the flux measurement from Super-Kamiokande. The daytime and nighttime fluxes and the flux for each 1.5 month interval over one year of data-taking are also discussed.

Super-Kamiokande, the first “second-generation” solar neutrino experiment, started operation on April 1st, 1996. Located at a depth of 2700 meters water equivalent in the Kamioka Mozumi mine in Japan, the detector is a 50,000 ton imaging water Cherenkov detector and has a cylindrical geometry, 39.3 m in diameter and 41.4 m in height. The central 32,000 tons – 36.2 m in height and 33.8 m in diameter – is called the inner detector and is viewed by 11,146 50-cm photomultiplier tubes (PMTs) which cover 40% of the inner surface. Surrounding the inner detector is the outer detector, which comprises a 2.6 to 2.75 m thick layer of water. The outermost 2.15 m of this water is an active detector, viewed by 1,885 20-cm PMTs to identify in-coming particles. This also serves to passively reduce γ and neutron backgrounds from the rocks surrounding the detector. An inactive region of 0.6 m thickness separates the inner detector from the active part of the outer detector with black sheets which prevent light transmission between the two regions. A fiducial volume of 22,500 tons of water, about 70% of the inner volume, is used for the solar neutrino analysis; the outer edge of this fiducial volume is located 2 m from the surface of the inner detector. This gives 4.75 m of water outside of the fiducial volume – 13.2 radiation lengths and 7.9 nuclear collision lengths – a very thick shield against backgrounds from the rock.

Solar neutrinos produce electrons in the water through neutrino–electron elastic scattering, and subsequently the recoil electrons emit Cherenkov photons. These photons are then detected by the PMTs on the surface of the inner detector. The front-end electronics for each hit PMT creates a 200 ns wide pulse, and the hardware trigger is made via a simple sum of the number of hit PMT pulses. The trigger threshold for events used in this analysis, 29 hits within an approximately 200 ns coincidence window in excess of the continuous noise hits due to PMT dark noise, corresponds to about 5.7 MeV (total energy). The analysis threshold was set at 6.5 MeV, for which the hardware trigger is only 0.2% inefficient. The trigger rate during this period was stable at ~ 11 Hz.

Solar neutrino interactions are reconstructed by using the charge and timing data from the hit PMTs. Recoil electrons have a short range (< 8 cm) and their Cherenkov light effectively comes from a point. We use a grid search method to find the event vertex. First, hits to be used for the vertex search are selected by sliding a time window until maximum signal to background significance is obtained. Then the grid point which gives the best fit on a 4m fixed mesh is selected. Final refinement of the vertex position, down to a 6 cm step size, is also done by a grid search method. The direction of each event is obtained by a maximum likelihood technique which uses the relative direction of each hit PMT. For each event, the recoil electron energy is initially determined by the number of hit PMTs in a 50 ns time window, since most of the PMT hits for events in the energy range of interest are due to only one photoelectron. We make corrections to the number of hit PMTs in order to compensate for light attenuation through the water, bad PMTs, angular dependence of the acceptance, the effective density of PMTs, and the probability of a two photon hit on a PMT in order to get uniform response over the fiducial volume. We further correct for noise hits due to the PMT dark rate (~ 3.3 kHz) which contributes about 1.8 hits within 50 ns. The tail of the time distribution up to 100 ns, caused by scattering of light in the water and reflections on the surfaces of the PMTs and black sheet, is also corrected for. The resulting corrected number of hit PMTs, N_{eff} , is closely related to the energy of the events.

An electron linear accelerator (LINAC) is used for calibrating the absolute energy scale, angular resolution, and vertex position resolution. Details of the LINAC calibration will be described elsewhere; a brief summary of the calibration is given here. The LINAC, located near the Super-Kamiokande detector, injects mono-energetic electrons with a tunable energy ranging from 5 MeV to 16 MeV. This matches the energy of the solar neutrinos detected in Super-Kamiokande. The absolute energy of the beam is measured by a germanium detector, which was in turn calibrated by gamma-ray sources and internal-conversion electrons from a ^{207}Bi source; the uncertainty of the beam energy is less than 20 keV over the energy range covered by the LINAC. LINAC data were taken at 6 different positions in the Super-Kamiokande tank between December 1996 and October 1997[12].

A typical distribution of reconstructed electron energy and direction relative to the injected beam direction is shown in Fig.1 for an 8.86 MeV/c momentum beam together with that obtained by a Monte Carlo simulation. Parameters in the Monte Carlo program, mainly the photon scattering and absorption lengths in water, were tuned in such a way that the Monte Carlo reproduces the LINAC data at various positions and energies. The Monte Carlo calculations are used to extrapolate these calibrations to the entire fiducial volume and all directions.

The energy calibration by the LINAC is cross-checked using gamma-rays from $\text{Ni}(n,\gamma)\text{Ni}$ reactions. The absolute energy scale obtained by the $\text{Ni}(n,\gamma)\text{Ni}$ is produced by comparing the observed gamma-ray spectrum with a simulation based on a model of gamma transition; it is 1.4% lower than that obtained by the LINAC calibration. It is suspected that the difference is due to gamma-rays with small branching ratios in the $\text{Ni}(n,\gamma)\text{Ni}$ reaction and non-uniformity of the source. Hence, we use the $\text{Ni}(n,\gamma)\text{Ni}$ calibration only for determining the relative position dependence of the energy scale in the detector. The comparison of the position dependence between the LINAC and the $\text{Ni}(n,\gamma)\text{Ni}$ shows that the agreement is better than 0.5%. The absolute energy scale is also cross-checked using beta-decays of ^{16}N produced by cosmic ray stopping muons. The observed beta spectrum agrees with the Monte Carlo simulation to better than 1.5% within the statistical accuracy of the measurement.

Water transparency used as inputs for a Monte Carlo program was measured by a dye laser and a CCD camera. Since the water transparency varies slightly with time, we monitor and correct for the small changes by using the Michel spectrum of electrons originating from stopping muons. We observe

about 1,200 such events per day. Using this correction, we kept the peak of the Michel spectrum stable to within $\pm 0.5\%$. In addition, the time dependence of the peak energy of the γ -rays from the Ni-calibration after this correction is less than $\pm 0.5\%$. A similar check was also made by using muon induced spallation events and a similar result was obtained.

For the present analysis we have used the data obtained from 297.4 live days between 31 May 1996 and 23 June 1997. The detector live time fraction during this period was greater than 90%. Most of the down time was due to calibrations of the detector.

The data set consisting of $\sim 3 \times 10^8$ events was reduced using algorithms similar to those used in the Kamiokande experiment [2, 3]. This reduction process required that events be (1) contained, (2) low energy, and (3) separated by more than 20 μs from any previous trigger. The contained event cut required less than 20 hits in the outer detector and the low energy cut required that the event have less than 1000 photoelectrons (110~120 MeV). We applied noise cuts that are effective in removing backgrounds in the lower energy region below 7 MeV. One of the backgrounds in this region involves events which have small clustered hits, i.e., several hit PMTs located next to each other. It is suspected that these events may come from radioactive contamination in the PMT glass. These noise cuts reduced the background level by more than a factor of three between 6.5 MeV and 7 MeV while keeping more than 90% of the signal events in the same energy region. The efficiency for these cuts was obtained by Monte Carlo calculation and also by studying the effect on spallation events. An energy cut of 6.5 MeV yielded about 57 events/day/kton with an overall efficiency of 94.2%

The main source of the remaining background events is muon-induced spallation products. These decay products of fragmented ^{16}O nuclei can effectively mimic solar neutrino events. We identify them via a likelihood analysis on the variables: time from previous muon event; distance from previous muon track; and muon energy loss along that track. A cut on the likelihood function was chosen to optimize the effectiveness of the overall spallation cut, thereby yielding approximately the maximum significance for the solar neutrino signal/ $\sqrt{\text{background}}$. This reduced the event rate to 12 events/day/kton. Application of the spallation cut results in a dead time and a dead volume, which we treated in analysis as an effective dead time for the solar neutrino signal. This dead time was calculated to be 20% by using real muon data and distributing Monte Carlo low energy events randomly in space and time throughout the detector volume. The data was further reduced by removing the gamma-ray backgrounds from the rocks surrounding the detector, thus giving a final rate of 7.6 events/day/kton [2, 3].

The directional distribution to the Sun of events in the final data sample is shown in Fig. 2. The data was divided into 16 energy bins. The number of solar neutrino events was extracted from the binned data by a maximum likelihood method using angular distributions expected for the solar neutrino signal and a near-flat background distribution with small corrections made for a slight directional anisotropies in local detector coordinates [2, 3]. In this method, the ^8B solar neutrino spectral shape is assumed. We obtained $4017 \pm 105(\text{stat.})_{-116}^{+161}(\text{syst.})$ solar neutrino events between 6.5 MeV and 20 MeV. Using this number and assuming the ^8B solar neutrino energy spectrum [14], the total ^8B solar neutrino flux was calculated to be $2.42 \pm 0.06(\text{stat.})_{-0.07}^{+0.10}(\text{syst.}) \times 10^6/\text{cm}^2/\text{s}$, which is consistent with the Kamiokande flux of $2.80 \pm 0.19(\text{stat.}) \pm 0.33(\text{syst.}) \times 10^6/\text{cm}^2/\text{s}$. Using this flux measurement and the most recent SSM (BP95) calculation [6], which has gone up by 16% from BP92 [7], we get a Data/SSM of $0.358_{-0.008}^{+0.009}(\text{stat.})_{-0.010}^{+0.014}(\text{syst.})$ for the 6.5 MeV energy threshold data sample.

The largest of our systematic errors comes from the uncertainty of the angular resolution. The total systematic errors of $\pm 4.0\%$ include the uncertainty of the energy determination $\pm 2.3\%$, the uncertainty of the expected ^8B energy spectrum $\pm 1.2\%$, the uncertainty in trigger efficiency (+0.2%), the noise cuts ($\pm 0.7\%$), directional fit (+2.9%), data reduction ($\pm 0.2\%$), background shape ($\pm 0.1\%$), spallation dead time ($< 0.1\%$), fiducial volume (-1.3%), cross section ($\pm 0.5\%$), and live time calculation ($\pm 0.1\%$). The details of the systematic errors will be explained in [13].

Solar neutrino fluxes for different data sets were obtained. The number of events extracted above 7 MeV was $3362_{-88}^{+96}(\text{stat.})_{-101}^{+138}(\text{syst.})$ and the total flux from this data set is $2.44_{-0.06}^{+0.07}(\text{stat.})_{-0.07}^{+0.10}(\text{syst.}) \times 10^6/\text{cm}^2/\text{s}$. The flux for the smaller inner fiducial volume of 11.7 kton was $2.47_{-0.08}^{+0.09}(\text{stat.})_{-0.07}^{+0.10}(\text{syst.}) \times 10^6/\text{cm}^2/\text{s}$. Both are consistent with that obtained for the entire 22.5 kton fiducial volume above 6.5 MeV. The daytime and nighttime fluxes were measured separately. The daytime flux was $2.39 \pm 0.09(\text{stat.})_{-0.07}^{+0.10}(\text{syst.}) \times 10^6/\text{cm}^2/\text{s}$

and the nighttime flux was $2.44_{-0.08}^{+0.09}(\text{stat.})_{-0.07}^{+0.10}(\text{syst.}) \times 10^6/\text{cm}^2/\text{s}$. There is no significant difference seen between the daytime and nighttime fluxes. These fluxes are interesting for studying neutrino oscillations[9], and a detailed study and consideration of the implications of the day/night results will be published later.

Finally, the data were divided into subsets, each consisting of about 1.5 months of data where those divisions were determined by taking into account the date of Earth's perihelion (Jan-2) and aphelion (Jul-3) in its orbit around the Sun. In this way we are able to study the stability of the solar neutrino flux and look for possible seasonal effects, although the statistics have not yet reached the level needed to study the effect of the 'Just So' oscillation scenario[15, 9]. Fig. 3 shows that the flux was stable over a one year long period. The anticipated flux variation ($\sim 7\%$ maximum) due to the eccentricity of the Earth's orbit is shown by the solid line. The χ^2 for the solid line is 10.30 with 8 degrees of freedom.

We also performed an independent solar neutrino analysis [16] in addition to the Kamiokande-based analysis described here [17]. The two analyses had access to the same raw calibration data and both used the same raw data. All subsequent steps in the data processing, event reconstruction, and efficiency determination for the two analyses were different and were performed independently. The results from that analysis are in agreement with the flux measurement reported here. A detailed comparison will be presented in a future publication.

In summary, the Super-Kamiokande detector has observed a stable flux of solar neutrinos that is consistent with that reported by the Kamiokande experiment and is significantly lower than predicted by standard solar models. The implications of the day/night flux ratio and the spectrum of the recoil electron energy, both very important for the study of a possible neutrino mass, will be published later.

We gratefully acknowledge the cooperation of the Kamioka Mining and Smelting Company. This work was partly supported by the Japanese Ministry of Education, Science and Culture and the U.S. Department of Energy.

References

- [1] B.T.Cleveland et al., Nucl. Phys. B(Proc. Suppl.) 38, 47(1995); R.Davis, Prog. Part. Nucl. Phys. 32, 13(1994).
- [2] K.S.Hirata et al., Phys. Rev. Lett. 65, 1297(1990); K.S.Hirata et al., Phys. Rev. D44, 2241(1991); D45, 2170E(1992).
- [3] Y.Fukuda et al., Phys. Rev. Lett. 77,1683(1996).
- [4] J.N.Abdurashitov et al., Phys. Lett. B328, 234(1994).
- [5] P.Anselmann et al., Phys. Lett. B327, 377(1994); B342, 440(1995).
- [6] J.N.Bahcall and M.Pinsonneault, Rev. Mod. Phys. 67, 781(1995).
- [7] J.N.Bahcall and M.Pinsonneault, Rev. Mod. Phys. 64, 885(1992).
- [8] S.Turck-Chièze and I.Lopes, Ap. J. 408,347(1993).
- [9] See for example, N. Hata and P. Langacker, IASSNS-AST 97/29 for a recent review.
- [10] S.P.Mikheyev and A.Y.Smirnov, Sov. Jour. Nucl. Phys. 42, 913(1985); L.Wolfenstein, Phys. Rev. D17, 2369(1978).
- [11] L.B.Okun et al., Sov. J. Nucl. Phys. 44,440(1986); C.S.Lim and W.J.Marciano, Phys. Rev. D37,1368(1988); E.Kh.Akhmedov, Phys. Lett. B213, 64(1988).
- [12] Super-Kamiokande Collaboration, to be submitted.

- [13] Super-Kamiokande Collaboration, to be submitted.
- [14] J.N.Bahcall et al., Phys. Rev, D51, 6146(1995).
- [15] S.M.Bilenky and B.Pontecorvo, Phys. Rep. 41, 225(1978); V.Barger, R.J.N.Phillips and K. Whisnant, Phys. Rev. D24, 538 (1981); S.L.Glashow and L.Krauss, Phys. Lett. B190, 199(1987).
- [16] Z. Conner, Ph.D. Thesis, University of Maryland (1997).
- [17] Y. Koshio, Ph.D. Thesis, University of Tokyo (1998); H. Okazawa, Ph.D. Thesis, Niigata University (1998); T. Yamaguchi, Ph.D. Thesis, Osaka University (1998); R. Sanford, Ph.D. Thesis, Louisiana State University (1998).

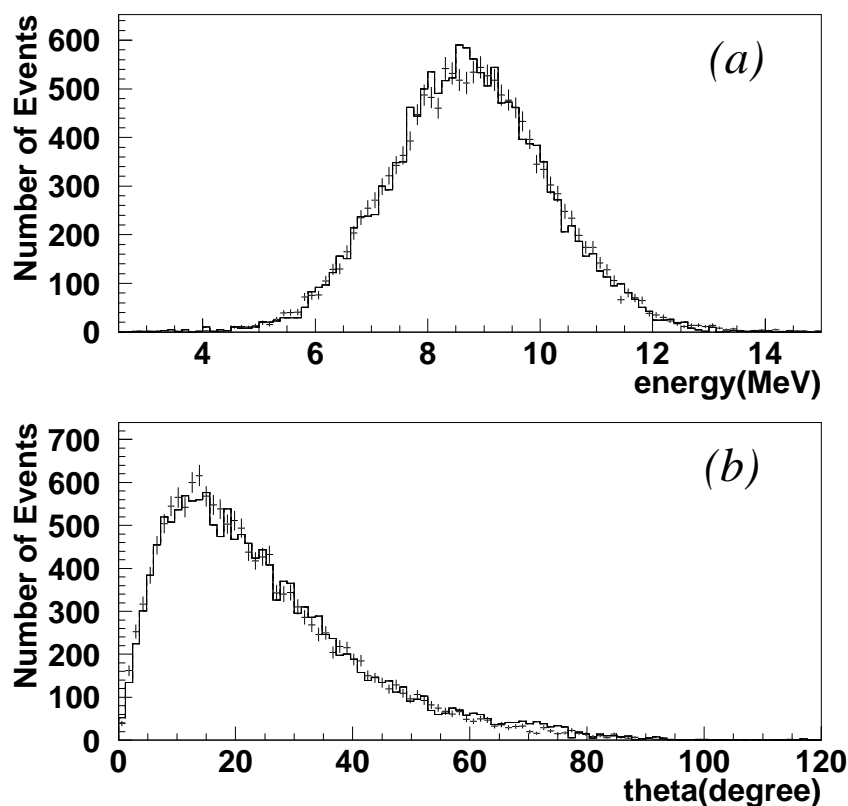


Figure 1: (a) A typical energy distribution of 8.86MeV electrons produced by the electron LINAC. (b) A typical angular distribution of 8.86MeV electrons produced by the electron LINAC. Also shown is that of the Monte Carlo electron events produced at the same vertex position.

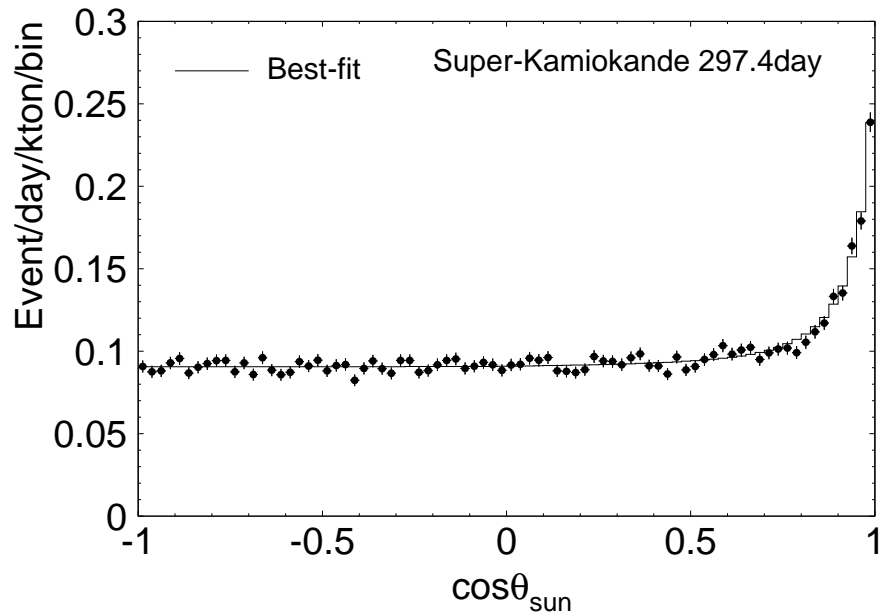


Figure 2: Plot of the cosine of the angle between the electron direction and a radius vector from the Sun. One obtains a clear peak from the solar neutrinos. The solid line shows the best fit to the data.

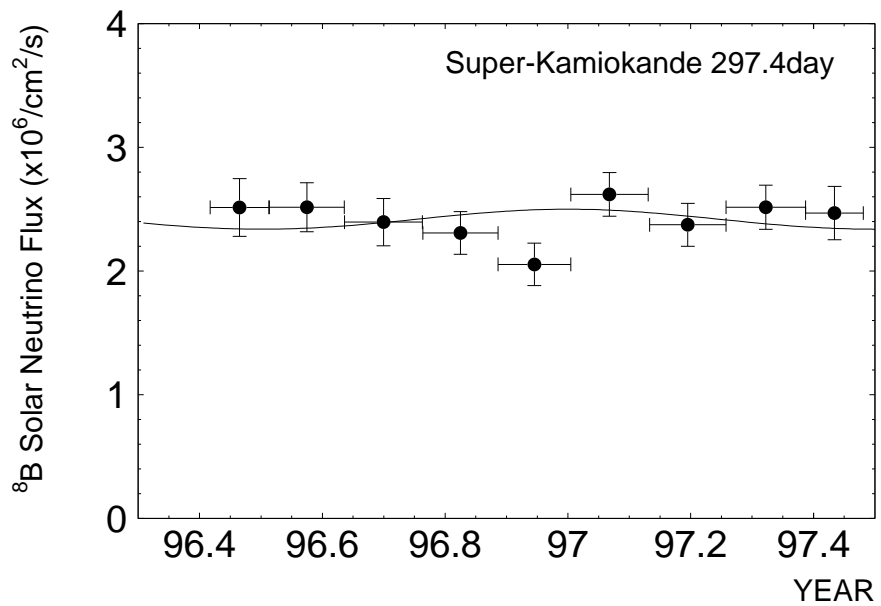


Figure 3: The flux in ~ 1.5 month periods from June 96 to June 97. The solid line shows the expected yearly change of the flux (about 7%) due to the eccentricity of the Earth's orbit around the Sun.